

# Force-Stroke Analysis of Metallic Materials using the Upper Bound Method

Kaan Ozel<sup>1,\*</sup>, Selcuk Selvi<sup>1</sup>, Mehmet Sahin<sup>2</sup>, Mumin Sahin<sup>1</sup>

Trakya University, Department of Mechanical Engineering, Faculty of Engineering, Edirne, Turkey<sup>1</sup>  
Kirkklareli University, Department of Mechanical Engineering, Faculty of Engineering, Kirkklareli, Turkey<sup>2</sup>  
E-mail: <sup>1</sup>kaanozel@trakya.edu.tr

**Abstract:** All plastic deformation applied to metallic materials create a metal flow. The main factors affecting metal flow are the friction conditions between the metallic material and the mold. In addition upset forces are closely related to the geometric shapes of the metallic materials that changes deformation rates. It is possible to express the formation rates with mathematical approaches in shaping metallic materials. However obtaining these mathematical approaches can be done with very complex methods. Numerical and analytical expressions are generally used in the mathematical approaches. Some of the approaches applied to obtain more accurate results are slip lines methods, finite elements analysis, finite difference methods and Boundary element methods. In this study the upper bound method was applied for metallic materials. The force-stroke diagrams were obtained by the investigation of deformation energy and friction losses. The analyzed parts were prismatic specimen with arbitrary profiles and the results obtained were supported by graphics.

**Keywords:** PLASTIC DEFORMATION, FORCE-STROKE ANALYSIS, UPPER BOUND METHOD

## 1. Introduction

Metal plastic shaping is a common process that has been done for many years. Upsetting is one of the most commonly used metal forming methods. It is based on the principle of changing the shape of the metals without changing their volume with the help of force and pressure. This application area, which is extremely important in industry and applications, can be done more easily with ductile materials that can be easily shaped. It means that the length of a stacked piece is shortened by the effect of the compressive force applied to it in the direction of its axis and the section is widened in the direction perpendicular to the direction of force. While the volume of the material does not change after upsetting, geometrical changes may occur in the material due to strain. The upsetting ratio is generally measured as the percentage reduction in length for cylindrical parts. Performing force analysis before the upsetting process positively affects the upsetting results. This prevents unexpected results and errors. In order to perform force analysis, the stamp force must be calculated depending on the upsetting rate. These calculations can be made thanks to some methods. One of these is the upper limit method, and this method can be applied to a part whose cylindrical coordinates are given. In the application of this method, stacking ratio and friction coefficients are taken as basis.

Gunasekera and Hoshino (1985) examined curvilinear profile molds to examine the extrusion of polygonal profile products. Curvilinear profile molds facilitate material flow and improve the forming process. Upper limit analysis was carried out for curvilinear profile and linear shrinking molds with 60% extrusion rate and 0.1 friction factor values and solution graphics were obtained. The results show that in curvilinear profile molds, the power component from plastic forming becomes dominant when the mold length decreases, and this force decreases suddenly when the mold length increases. In contrast, in straight shrinking dies the force component remains almost constant throughout forming. The study also revealed that the optimal pattern length of curvilinear patterns is shorter. The obtained theoretical results were confirmed by experiments with lead samples at room temperature. The result shows that dies with curvilinear profiles are more efficient and effective in extrusion processes [1].

Yang, D.Y., et al. (1986) stated in their study that in molds with inlet and outlet sections of different profiles, it is difficult to make the analytical expression of the mold surface connecting these sections in cylindrical coordinates. The study aims to solve this problem by proposing a transition function  $R(\theta,0)$  and  $R(\theta,L)$  that defines the input and output sections as  $R(\theta,z)$ , respectively. The transition function was chosen to define the input section for  $z=0$  and the output section for  $z=L$  and was obtained using a certain number of Fourier series. Thanks to this transition function, a new velocity field was defined and the results obtained for exit profiles

with elliptical and rectangular cross-sections were compared with experimental data using the Al 2024 material, using the upper limit method. The results showed that the surface quality of the resulting products was quite good. It was also observed in the study that the results obtained with the upper bound method were slightly higher than the experimental results. This difference is partly due to the fact that the profile with a square cross-section has a larger circumferential length of the surrounding circle than the elliptical profile, requiring more energy for shaping. This study improved the definition of the transition function and verified the results obtained by the upper bound method through experiments [2].

In this study, Narayanasamy et al. (2006) obtained the results of the transition from circular billet to circular cross-section exit profile and cosine profile patterns using the upper limit method and examined them compared to previous studies. The upper limit analysis was made by expressing the path between the particle's mold entry and exit profiles as a function in the Cartesian coordinate system, and the velocity fields were calculated through this function. This method has been used to predict plastic deformation. When the results obtained in the study were compared with the calculations of flat shrinking molds and convex circular molds under frictionless conditions, it was found that the cosine profile required lower extrusion pressure and was therefore more advantageous than other molds. In addition, calculations made with similar die profiles are presented graphically according to relative extrusion pressure and die length changes, with power amount comparisons made using a flat shrinking matrix. According to these comparisons, it has been shown that cosine transition profiles have lower amounts of power spent for plastic deformation and friction, and this power is less for each value according to the mold length [3].

Bakhshi-Jooybari, M. et al (2007) proposed a new approach combining cap and slice method to estimate strength in cold extrusion of aluminum and lead samples. In the study conducted with this method, the authors used conical molds they had previously designed for comparison purposes. The results obtained with the proposed new method were compared with experimental data and solutions obtained with the commercial finite element software. When the experimental force-stroke diagrams were examined, it was observed that the combined method was compatible with simulation and experimental results. Additionally, it was determined that when the optimum curvilinear die was used for aluminum and lead samples, the required force was lower than when the optimum conical die was used. This result indicates that the forming process requires less energy with optimum curvilinear molds compared to conical molds and confirms the accuracy of finite elements and experimental results [4].

Ebrahimi, R. (2008) and his team developed a new upper bound analysis method for tube extrusion. The authors compared the optimum die half angle obtained with numerical and analytical

solutions. They stated that at a constant friction factor value, there is an optimum angle that minimizes the power required for the forming process. They used a separate equation to calculate this optimum die angle. They found that as the friction factor increases, the die half angle also increases, but the constant friction factor does not have any effect on the dead metal zone angle. They also observed that when the extrusion rate increased, the optimum die half angle also increased. They emphasized that the effect of extrusion rate is more evident at high friction factor values [5].

Abrinia, K. and Makaremi, M. (2009) developed a new design and analysis method to model material flow with expanding square, rectangular and elliptical cross-sections. The molds they choose are designed to allow material to flow towards the lateral surfaces. They examined molds with various extrusion rates and investigated the effects of parameters such as friction effect and extrusion rate on extrusion pressure. While they used the upper limit analysis method to determine the maximum extrusion pressure, they preferred the finite element method to facilitate mold design. In their experiments to verify the theory, they demonstrated that the experimental, numerical and theoretical results were compatible and that these methods could be used for scattering patterns. Their proposed upper bound analysis method involves a kinematically new velocity field and has been used to estimate the maximum energy required for forming. In the experiments, commercially pure lead material and different mold sets were used [6].

Shu-peng C. and Zhong-jin W. (2020) represented the upset forging process of three-dimensional elliptical disks and rings was analyzed using the upper bound method. A general form of kinematically valid velocity fields is proposed with three control functions, each containing a free parameter. In this way, factors such as sideways spreading, lateral swelling in the thickness direction and movement of the neutral surface that occurred during the "upset" forging process of the ellipse rings could be taken into account. It has been shown that by choosing different control functions in the proposed general form, kinematically valid velocity fields suggested by other researchers in previous references can be obtained. By optimizing the free parameters with the simplex algorithm in the upper bound method, the forging load and the shapes of the workpiece in the deformation stages could be calculated. Calculations made for different workpiece shapes and friction conditions show that the theoretical results obtained are compatible with the experimental results in previous studies and the finite element analysis performed in this study [7].

Hamed A. (2022) has worked on a new mathematical model is developed to predict the gap closing behavior of metal rods during the plane strain extrusion process. For this purpose, an improved upper bound analysis has been carried out by applying the power balance between the intrinsic work rate, the rate of energy release across the gap, and the extrinsic force. Considering the limiting condition of the resulting equations at the gap closure threshold, a mechanical criterion was obtained to find the minimum extrusion rate required for the closure of elliptical gaps. The formulation was developed for frictionless and frictional conditions at the die-rod interface. Additionally, the process was modeled with the finite element method (FEM) and it was observed that the obtained analytical criterion and FEM modeling provided a good match in terms of minimum required extrusion rate. It is found that the minimum extrusion rate required to close the voids is solely a function of the extrusion die angle, the void aspect ratio, and the friction condition at the die-rod interface. Additionally, it has been determined that extruding the material under frictional conditions and with a die with a smaller taper angle is beneficial in closing the gaps [8].

Khanlari H. and Honarpisheh M. (2023) published a study on the upper limit (UB) analysis of the channel angular printing process was carried out by taking into account the die angle, the thickness of the entry and exit channels, the outer and inner corner radii, the die geometric properties such as the length of the exit channel and the length of the first workpiece, friction and strain

hardening of the material, under cold conditions and for a rectangular cross-section workpiece. In order to verify the results of the UB analysis, the results of the analytical equations were compared with the numerical simulation and the real process. The results revealed that decreasing the die angle, the thickness of the exit channel and the outer corner radius, and increasing the thickness of the entrance channel and the inner corner radius increased the total plastic stress and processing force. Moreover, it has been shown that the processing force increases with increasing the initial workpiece length. A very good agreement was achieved between the analytical method and the results of the numerical and experimental methods [9].

In hot and cold upsetting processes, if lubrication is very sufficient, the friction force will be close to zero. If the object on which the upsetting process is applied is a cylinder, when each part of the cylinder is divided into small elements, it is seen that the deformation between the elements is equal. Due to volume constancy, there is no volumetric change while the cylinder decreases in length.

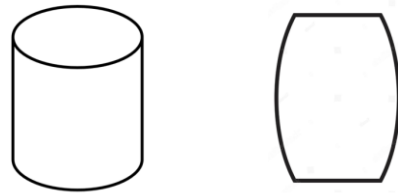


Fig. 1 Cylindrical parts before and after in the upsetting process.

## 2. Upper Bound Analysis Method

In order to calculate the total power consumption in the upper bound method analysis, it is necessary to take into account the total of all energy consumed. The total power consumption is obtained by calculating the power consumption of each process in which energy is consumed separately. Thus, the upper limit for total power consumption is found [10,11].

$J^*$ : Upper bound for total power consumption

$$J^* = \sum \dot{W}_t + \sum \dot{W}_s + \sum \dot{W}_f \quad (1)$$

$\dot{W}_i$ : Ideal deformation power

$$\dot{W}_i = \bar{\sigma}_m^{(l)} \int \dot{\epsilon} dV \quad (2)$$

$\dot{\epsilon}$ : Effective strain velocity

$$\dot{\epsilon} = \frac{2}{\sqrt{3}} \left( \frac{1}{2} (\dot{\epsilon}_r^2 + \dot{\epsilon}_\theta^2 + \dot{\epsilon}_z^2) + \dot{\epsilon}_{r\theta}^2 + \dot{\epsilon}_{\theta z}^2 + \dot{\epsilon}_{rz}^2 \right)^{1/2} \quad (3)$$

$\bar{\sigma}_m^{(j)}$ : Effective stress value

$$\bar{\sigma}_m^{(j)} = \frac{1}{\bar{\epsilon}_f^{(j)}} \int_0^{\bar{\epsilon}_f^{(j)}} \sigma d\epsilon \quad (4)$$

$\bar{\epsilon}_f^{(j)}$ : Effective strain value

$$\bar{\epsilon}_f^{(j)} = \sum_{i=1}^j \ln \left( \frac{H^{(i)}}{H^{(i-1)}} \right) \quad (5)$$

$\dot{W}_f$ : Friction power between the mold and the part

$$\dot{W}_f = \frac{m}{\sqrt{3}} \bar{\sigma}_m^{(l)} \int_{S_f} |\Delta V| ds \quad (6)$$

$P_{avg}$ : Average stamp pressure

$$P_{avg} = \frac{J^*}{A_r U_0} \quad (7)$$

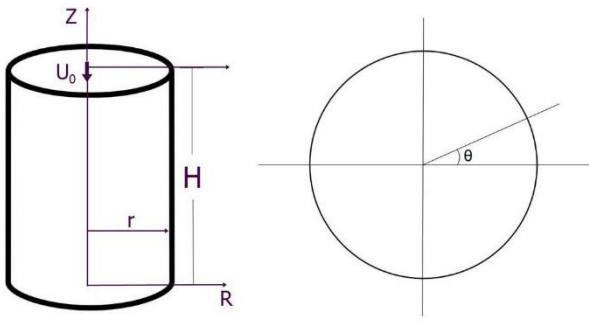


Fig. 2 Cylindrical coordinates of upsetting part.

### 3.1. Distribution of Kinematic Velocity Elements

The velocity elements occurring for an object whose cylindrical coordinates are given are  $U_z$ ,  $U_\theta$ ,  $U_r$  in order and their mathematical expressions are as follows [7,8].

$U_z$ : Axial velocity equation

$$U_z = \frac{-U_0 Z}{T} \quad (8)$$

$U_\theta$ : Tangential velocity equation

$$U_\theta = \frac{-U_0 R}{T} \omega_1(\theta) \quad (9)$$

$$\omega_1(\theta) = \frac{(a-b)}{(a+b)} D_1 \sin(2\theta) \quad (10)$$

$$\omega_1(\theta) = \frac{(a-a)}{(a+a)} D_1 \sin(2\theta) = 0 \quad (11)$$

$$U_\theta = \frac{-U_0 R}{T} \omega_1(\theta) = \frac{-U_0 R}{T} \cdot 0 = 0 \quad (12)$$

$$U_\theta = 0 \quad (13)$$

$U_r$ : Radial velocity equation

$$U_r = \frac{U_0 R}{2T} \cdot \left(1 + \frac{d\omega_1(\theta)}{d\theta}\right) \quad (14)$$

$$U_r = \frac{U_0 R}{2T} \cdot (1 + 0) = \frac{U_0 R}{2T} \quad (15)$$

$$U_r = \frac{U_0 R}{2T} \quad (16)$$

### 3. Force Analysis for Cylindrical Prism

The expressions of the velocity components occurring on the material are given in the equations below:

$$U_z = \frac{-U_0 Z}{T} \quad (17)$$

$$U_\theta = \frac{-U_0 R}{T} \omega_1(\theta) \quad (18)$$

Since  $b = a$  in cylindrical materials, equations are shown as follows:

$$\omega_1(\theta) = \frac{(a-b)}{(a+b)} D_1 \sin(2\theta) \quad (19)$$

$$\omega_1(\theta) = \frac{(a-a)}{(a+a)} D_1 \sin(2\theta) = 0 \quad (20)$$

$$U_\theta = \frac{-U_0 R}{T} \omega_1(\theta) = \frac{-U_0 R}{T} \cdot 0 = 0 \quad (21)$$

$$U_\theta = \frac{-U_0 R}{T} \omega_1(\theta) = \frac{-U_0 R}{T} \cdot 0 = 0 \quad (22)$$

$$U_\theta = 0 \quad (23)$$

$$U_r = \frac{U_0 R}{2T} \cdot \left(1 + \frac{d\omega_1(\theta)}{d\theta}\right) \quad (24)$$

$$U_r = \frac{U_0 R}{2T} \cdot (1 + 0) = \frac{U_0 R}{2T} \quad (25)$$

$$U_r = \frac{U_0 R}{2T} \quad (27)$$

Since the volume does not change in compressed materials, based on the principle of volume constancy, strain rates are given by the following equations.

$$\frac{\partial U_r}{\partial R} + \frac{U_r}{R} + \frac{1}{R} \cdot \frac{\partial U_\theta}{\partial \theta} + \frac{\partial U_z}{\partial Z} = 0 \quad (28)$$

$$\dot{\epsilon}_r = \frac{\partial U_r}{\partial R} \quad (29)$$

$$\dot{\epsilon}_r = \frac{\partial U_r}{\partial R} = \frac{U_0}{2T} \quad (30)$$

$$\dot{\epsilon}_r = \frac{U_0}{2T} \quad (31)$$

$$\dot{\epsilon}_\theta = \frac{U_r}{R} + \frac{1}{R} \cdot \frac{\partial U_\theta}{\partial \theta} \quad (32)$$

$$\dot{\epsilon}_\theta = \frac{U_r}{R} + \frac{1}{R} \cdot \frac{\partial U_\theta}{\partial \theta} = \frac{U_0}{2T} + \frac{1}{R} \cdot 0 = \frac{U_0}{2T} \quad (33)$$

$$\dot{\epsilon}_\theta = \frac{U_0}{2T} \quad (34)$$

$$\dot{\epsilon}_z = \frac{\partial U_z}{\partial Z} \quad (35)$$

$$\dot{\epsilon}_z = \frac{\partial U_z}{\partial Z} = -\frac{U_0}{T} \quad (36)$$

$$\dot{\epsilon}_z = -\frac{U_0}{T} \quad (37)$$

Since the total deformation force must be found by taking all equations into consideration, mathematical operations are continued as follows:

$$J^* = \sum \dot{W}_t + \sum \dot{W}_s + \sum \dot{W}_f \quad (38)$$

$\dot{W}_t$  is the ideal deformation power:

$$\dot{W}_t = \bar{\sigma}_m^{(l)} \int \dot{\epsilon} dV \quad (39)$$

$$\dot{\epsilon} = \frac{2}{\sqrt{3}} \left( \frac{1}{2} (\dot{\epsilon}_r^2 + \dot{\epsilon}_\theta^2 + \dot{\epsilon}_z^2) + \dot{\epsilon}_{r\theta}^2 + \dot{\epsilon}_{\theta z}^2 + \dot{\epsilon}_{zr}^2 \right)^{1/2} \quad (40)$$

$$\dot{W}_t = \bar{\sigma}_m^{(j)} \int \dot{\epsilon} dV = \bar{\sigma} \iiint \frac{2}{3} \left( \sqrt{\frac{1}{2} (\dot{\epsilon}_r^2 + \dot{\epsilon}_\theta^2 + \dot{\epsilon}_z^2) + \dot{\epsilon}_{r\theta}^2 + \dot{\epsilon}_{\theta z}^2 + \dot{\epsilon}_{zr}^2} \right) r dr d\theta dz \quad (41)$$

$$\dot{W}_t = \pi R^2 \bar{\sigma} U_0 \quad (42)$$

$\dot{W}_f$  indicates power consumed due to friction between die and the stamp resulting in :

$$\dot{W}_f = \frac{m}{\sqrt{3}} \bar{\sigma}_m^{(l)} \int_{S_f} |\Delta V| ds \quad (43)$$

$$\dot{W}_f = \frac{m}{\sqrt{3}} \bar{\sigma}_m^{(l)} \int_{S_f} |\Delta V| ds = \frac{m}{\sqrt{3}} \bar{\sigma} \iint \sqrt{U_r^2 + U_\theta^2} r dr d\theta \quad (44)$$

$$\dot{W}_f = 2\pi R^3 \bar{\sigma} m \frac{U_0}{3\sqrt{3}T} \quad (45)$$

$\dot{W}_s$  is the amount of power consumption due to shear:

$$\dot{W}_s = 0 \quad (46)$$

$$J^* = \dot{W}_t + \dot{W}_f = \pi R^2 \bar{\sigma} U_0 + 2\pi R^3 \bar{\sigma} m \frac{U_0}{3\sqrt{3}T} \quad (47)$$

$$J^* = \pi R^2 \bar{\sigma} U_0 \left(1 + \frac{2}{3} \frac{m R}{\sqrt{3} T}\right) \quad (48)$$

$$J^* = \text{Force} * \text{Velocity} = F U_0 \quad (49)$$

$$F = \text{Area} * \text{Pressure} = \pi R^2 P_{avg} \quad (50)$$

$$J^* = \pi R^2 P_{avg} U_0 \quad (51)$$

$$J^* = \pi R^2 P_{avg} U_0 = \pi R^2 \bar{\sigma} U_0 \left(1 + \frac{2}{3} \frac{m R}{\sqrt{3} T}\right) \quad (52)$$

$$\frac{P_{avg}}{\bar{\sigma}} = 1 + \frac{2}{3} \frac{m R}{\sqrt{3} T} \quad (53)$$

Total upsetting force is,

$$F = \pi R^2 \bar{\sigma} \left(1 + \frac{2}{3} \frac{m R}{\sqrt{3} T}\right) \quad (54)$$

### 4. Calculations and Results

All theoretical calculations are given in the equations shown above. In the next stage, dimensional changes will be calculated and the results will be examined. In the figure below, the main axis and spare axis lengths of the ellipse are indicated as a and b respectively.

The dimensions of the cylindrical part are shown as a and b before the process, and as a<sub>1</sub> and b<sub>1</sub> after the process.

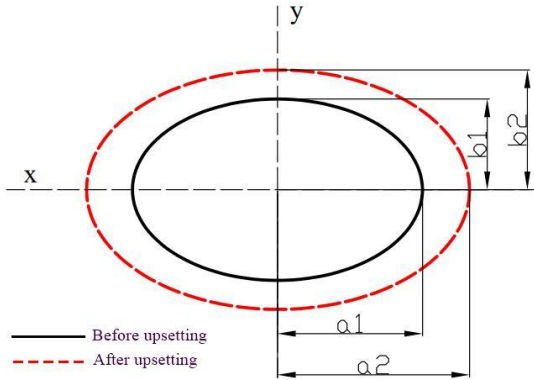


Fig. 3 Surface changes before and after upsetting on a cylindrical part.

$$\frac{a}{b} = \lambda = \frac{a_1}{b_1} = \frac{a_2}{b_2}$$

$$V = \pi \cdot a \cdot b \cdot h$$

$$V = \pi \cdot a_1 \cdot b_1 \cdot h_1 = \pi \cdot a_2 \cdot b_2 \cdot h_2$$

$$b_2 = \sqrt{\frac{a_1 \cdot b_1 \cdot h_1}{h_2 \cdot \lambda}}$$

The values resulting from calculations for different upsetting rates are shown in the table below.  $\dot{W}_i$  and  $\dot{W}_f$  values were found separately and then the total power  $J^*$  was calculated.

For the friction and deformation power requirements that occur when upsetting is applied at different rates to a cylindrical object with a height of 20 units and a radius of 30 units, which is taken as an example to examine the results after theoretical calculations, are shown below in the graphics for two different upsetting ratios.

Table 1: Lengths obtained according to %10 upsetting rates.

a <sub>1</sub>	b <sub>1</sub>	h <sub>1</sub>	h <sub>2</sub>	b <sub>2</sub>	a <sub>2</sub>
30	30	20	20	30	30
30	30	20	18	31,6227766	31,6227766
30	30	20	16	33,54101966	33,54101966
30	30	20	14	35,85685828	35,85685828
30	30	20	12	38,72983346	38,72983346
30	30	20	10	42,42640687	42,42640687
30	30	20	8	47,4341649	47,4341649

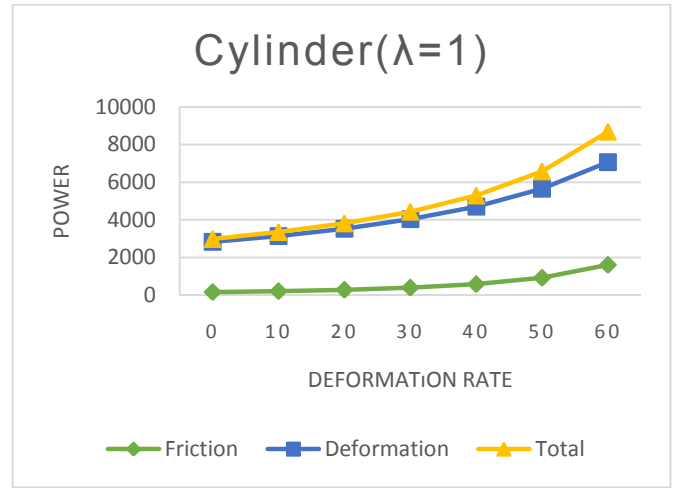


Fig. 4 Graphic for the %10 upsetting rates of cylindrical prism.

Table 2: Lengths obtained according to %5 upsetting rates.

a <sub>1</sub>	b <sub>1</sub>	h <sub>1</sub>	h <sub>2</sub>	b <sub>2</sub>	a <sub>2</sub>
30	30	20	20	30	30
30	30	20	19	30,77935056	30,77935056
30	30	20	18	31,6227766	31,6227766
30	30	20	17	32,53956867	32,53956867
30	30	20	16	33,54101966	33,54101966
30	30	20	15	34,64101615	34,64101615
30	30	20	14	35,85685828	35,85685828

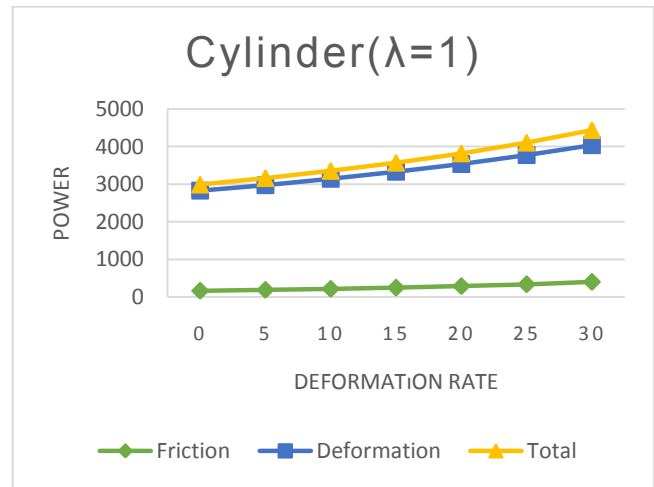


Fig. 5 Graphic for the %5 upsetting rates of cylindrical prism.

### 5. Results and Discussion

When all the results are examined, when upsetting is applied to a metallic object, the required power varies depending on the upsetting rate applied. In compression at high rates, more power is required for both friction and deformation. As the ratio of diameter to height increases, both amounts of power to be applied increase logarithmically. The aim of this study is to pre-calculate the appropriate conditions and the required amount of power when applying upsetting to cylindrical metals. With the results of the study, the theoretically intended numerical values were reached.

## 6. References

1. JS. Gunasekera, S. Hoshino, *Analysis of Extrusion of Polygonal Sections Through Streamlined Dies*, Journal of Eng. Tech., **107**, pp.229-233 (1985).
2. D.Y. Yang, C.H. Han, M.U. Kim, *A Generalized Method For Analysis Of Three-Dimensional Extrusion Of Arbitrarily-Shaped Sections*, Int. Jour. of Mech. Sciences, **28**, pp.517-534(1986).
3. R. Narayanasamy, R. Ponalagusamy, R. Venkatasen, P. Srinivasan, *An Upper Bound Solution to Extrusion of Circular Billet to Circular Shape Through Cosine Dies*, Matr. and Design, **27**, pp.411-415 (2006).
4. M. Bakhshi-Jooybari, M. Saboori, M. Noorani-Azad, S.J. Hosseinipour, *Combined Upper Bound and Slab Method Finite Element and Experimental Study Of Optimal Die Profile in Extrusion*, Matr. and Desg., **28**, pp.229-233 (2007).
5. R. Ebrahimi, M. Reihanian, M. Kanaani, M.M. Moshkar, *An Upper-Bound Analysis of the Tube Extrusion Process*, Journal of Matr. Process. Tech. , **199**, pp.214-220 (2008).
6. K. Abrinia, M. Makaremi, *An Analytical Solution for the Spread Extrusion of Shaped Sections*, Int. Journal of Adv. Manf. Tech., **41**, pp.670-676 (2009).
7. Shu-peng C., Zhong-jin W. *An analysis for three-dimensional upset forging of elliptical disks and rings based on the upper-bound method*, , Int. Journal of Mech. Sci., **183**, 105835 (2020)
8. Hamed A., *An improved upper bound analysis for study of the void closure behavior in the plane strain extrusion*, Mech. Resc. Commn., **124**, 103971 (2022)
9. Khanlari H., Honarpisheh M., *An upper bound analysis of channel angular pressing process considering die geometric characteristics, friction, and material strain-hardening*, CIRP Jour. of Manf. Sci. and Tech., **41**, pp.259-276 (2023)
10. W.B. Bae, D.Y. Yang, *An Upper-Bound Analysis of the Backward Extrusion of Tubes of Complicated Internal Shapes From Round Billets*, J. Mater. Process Tech., **36**, pp.157-173 (1993)
11. W.B. Bae, D.Y. Yang, *An Upper-Bound Analysis of the Backward Extrusion of Internally of Elliptic-Shaped Tubes From Round Billets*, J. Mater. Process Tech., **30**, pp.13-30 (1992)